Supplementary data

Effect of mono- and divalent extra-framework cations on the structure and accessibility of porosity in chabazite zeolites

Huan V. Doan,[*a,b] Ka Ming Leung,[c] Valeska P. Ting[*d] and Asel Sartbaeva[*e]

[a.] *School of Chemistry, University of Bristol, Bristol BS8 1TS, UK.*

[b.] *Department of Oil Refining and Petrochemistry, Hanoi University of Mining and Geology, Duc Thang, Bac Tu Liem, Hanoi, Vietnam.*

[c.] *Department of Chemistry, The University of Hong Kong, Pokfulam, Hong Kong SAR, China.*

[d.] *Department of Mechanical Engineering, University of Bristol, Bristol BS8 1TR, UK.*

[e.] *Department of Chemistry, University of Bath, Bath BA2 7AY, UK.*

*Corresponding authors. *Email: huan.doan@bristol.ac.uk (HVD); v.ting@bristol.ac.uk (VPT) and a.sartbaeva@bath.ac.uk (AS)*

Contents

1. Characterisation techniques 2

1.1. Scanning electron microscopy and energy-dispersive X-ray spectroscopy 2

1.2. Powder X-ray diffraction 2

1.3. Simulation using CrystalMaker and CrystalDiffract 2

1.4. Cell parameters analysis 3

1.5. Solid state magic angle spinning nuclear magnetic resonance 4

1.6. Gas sorption 4

2. Additional information and results 5

2.1. Cell parameters 5

2.2. Energy-dispersive X-ray spectroscopy 5

2.3. Simulation using CrystalMaker and CrystalDiffract 6

2.4. Solid state magic angle spinning nuclear magnetic resonance 7

2.5. Gas sorption 9

2.6. Powder X-ray diffraction of exchanged chabazite zeolites after gas sorption 9

1. Characterisation techniques

1.1. Scanning electron microscopy and energy-dispersive X-ray spectroscopy

Low resolution micrographs were taken using a JEOL SEM6480LV scanning electron microscope (SEM) with back scattering electrons (BSE). Energy-dispersive X-ray spectroscopy (EDX) data were acquired using an Oxford INCA X-ray analyser attached to the microscope. High resolution micrographs were taken using the JEOL FESEM6301F field emission scanning electron microscope at the University of Bath. Source: cold cathode UHV field emission conical anode gun, accelerating voltage: 5 - 20 kV, magnification from 10.000 times to 40.000 times.

1.2. Powder X-ray diffraction

Room temperature Powder X-ray diffraction (PXRD) results below were obtained using a BRUKER AXS D8-Advance with Vantec-1 detector using Cu Kα (λ = 1.5418 Å) as the source of X-ray radiation, in flat plate geometry with a spinner speed is 15 rpm, at the Department of Chemistry, University of Bath.

1.3. Simulation using CrystalMaker and CrystalDiffract

Crystal structures of chabazite zeolites were simulated in CrystalMaker for Windows (Version 9.1.4 (633), licensed to the University of Bath: Serial number: 2930) according to the data of Calligaris *et al.*,[1] space group is r$\bar{3}$m $a = b = c = 9.459$Å; $\alpha = \beta = \gamma = 94.07^{o}$. The atomic positions used are given in Table S1. The powder diffraction patterns of simulated samples were then compared with that of synthesised ones in CrystalDiffract for Window version 6.5.0 (211) licensed to University of Bath (serial number: 1166) to confirm the presence of cations in chabazite zeolites.

Table S1. Atomic positions used for simulation of chabazite structure

Label	Site Occupancy	x	y	z
Si	Si 0.67 Al 0.33	0.1033	0.3331	0.8743
O1	O 1.00	0.2665	-0.2665	0.0000
O2	O 1.00	0.1506	-0.1506	0.5000
O3	O 1.00	0.2503	0.2503	0.8930
O4	O 1.00	0.0204	0.0204	0.3193
K1	K 0.97	0.2222	0.2222	0.2222
K2	K 0.15	0.5611	0.5611	0.2506
K3	K 0.22	0.5255	0.5255	0.1064

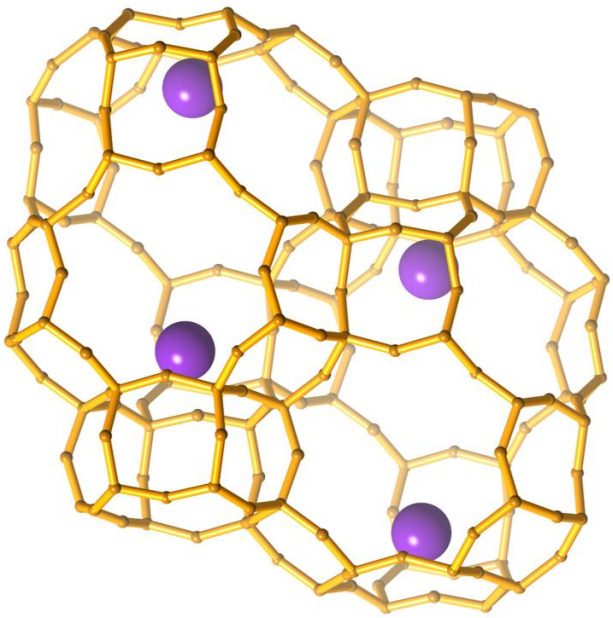

Figure S1. Crystal structure of K-CHA. Potassium atoms are presented by purple balls. Images generated using CrystalMaker®: a crystal and molecular structures program for Windows. CrystalMaker Software Ltd, Oxford, England

1.4. Cell parameters analysis

Le Bail analysis was performed on the diffraction spectra to calculate the cell parameters of synthesised chabazite samples. In each analysis, PXRD data (.xy file) and CHA structure (as shown in Table S1) were loaded in MAUD program[2] using the following setting, angular calibration: instrument misalignment, geometry: Bragg-Brentano, instrument broadening:

Caglioti PV, Size-Strain model: Anisotropic. Each structure was refined until the weighted profile R-factor (R_{wp}) value was below 18. An example of a refined XRD structure is given in Figure S2.

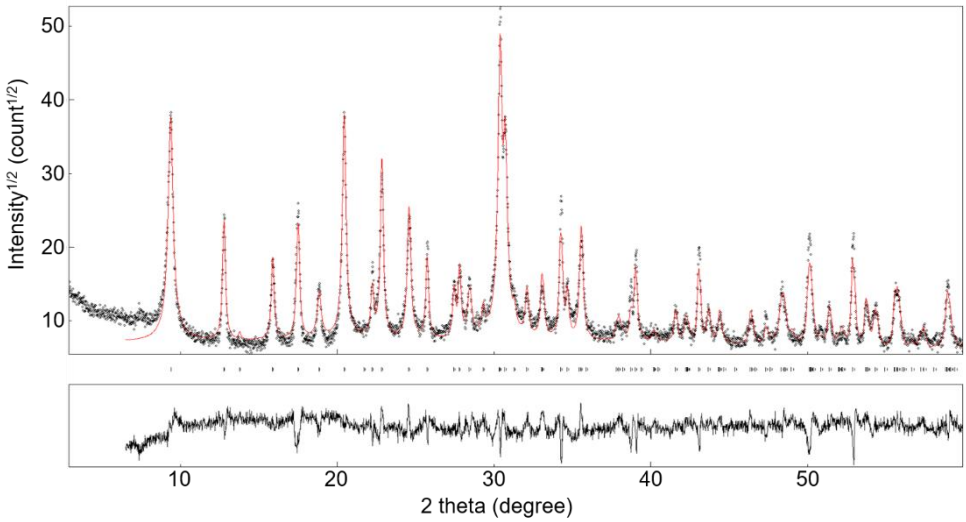

Figure S2: Refined PXRD patterns of KNaCHA

1.5. Solid state magic angle spinning nuclear magnetic resonance

^{29}Si and ^{27}Al NMR spectrum of chabazite zeolites were measured using a VARIAN VNMRS 400 spectrometer using direct excitation (DE) method, with tetramethylsilane and 1M aqueous aluminium nitrate solution as references. The spinning rate of ^{29}Si NMR was 6.8 kHz, ^{27}Al NMR was 14 kHz. Solid state NMR spectra were obtained at the EPSRC UK National Solid-state NMR service at Durham University. The data then were fitted using Solver program in Excel to a Pseudo-Gaussian function.

1.6. Gas sorption

The surface area of all chabazite zeolites in this research were determined on samples of ~100 mg using nitrogen sorption at 77 K with a Micromeritics 3-Flex volumetric gas sorption analysis system. Nitrogen was purchased from Air Products with purity of 99.9999%. Samples were degassed at 350 °C under dynamic high (10^{-6} mbar) vacuum for 12 h prior to analysis.

2. Additional information and results

2.1. Cell parameters

Table S2. Cell parameters of synthesised chabazite zeolites

Rhombohedral setting (r$\bar{3}$m)	KNA-CHA	Cs-CHA	Ca-CHA	Ba-CHA	Sr-CHA	Zn-CHA
a (Angstrom)	9.461	9.463	9.437	9.449	9.438	9.445
alpha (degree)	94.029	94.217	94.202	94.270	93.863	94.676

2.2. Energy-dispersive X-ray spectroscopy

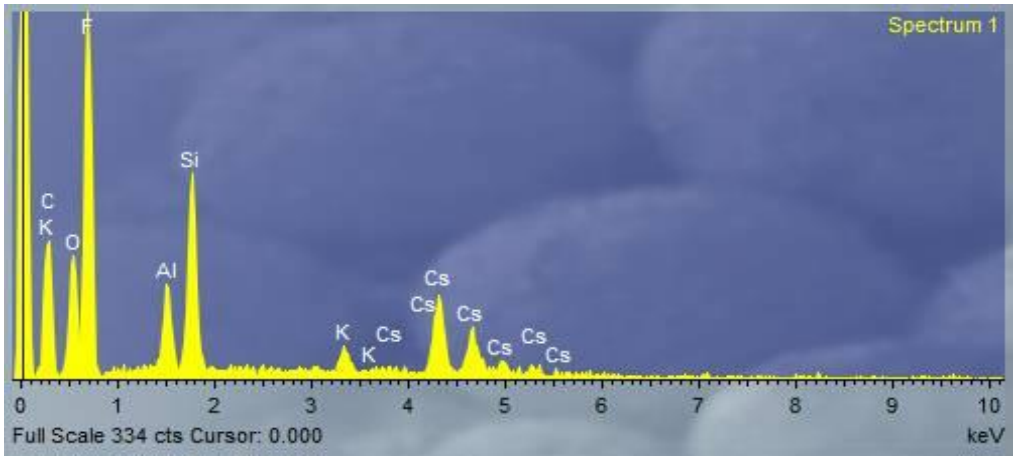

Figure S3. EDX spectrum of Cs-CHA

Table S3. The elemental composition of synthesised chabazite zeolites (atomic%)

Samples	O	Na	Al	Si	K	Cs	Ca	Sr	Ba	Zn
KNa-CHA	61.81 ±4.00	0.10 ±0.12	8.63 ±0.60	18.99 ±1.60	10.46 ±2.60	-	-	-	-	-
K-CHA	65.38 ±4.04	-	8.15 ±0.70	18.23 ±1.98	8.24 ±1.40	-	-	-	-	-
Cs-CHA	56.83 ±7.98	-	9.19 ±0.70	21.93 ±2.08	2.70 ±1.16	9.36 ±4.76	-	-	-	-
Ca-CHA	69.08 ±3.14	-	8.08 ±0.8	17.62 ±2.05	2.30 ±0.43	-	2.93 ±0.32	-	-	-
Sr-CHA	65.79 ±3.44	-	8.95 ±0.83	19.69 ±2.01	2.31 ±0.31	-	-	3.26 ±0.42	-	-
Ba-CHA	64.94 ±2.29	-	9.03 ±0.39	19.68 ±1.04	2.38 ±0.56	-	-	-	3.96 ±0.61	-
Zn-CHA	66.94 ±5.55	-	8.39 ±0.87	18.37 ±2.56	4.03 ±1.23	-	-	-	-	2.26 ±0.91

2.3. Simulation using CrystalMaker and CrystalDiffract

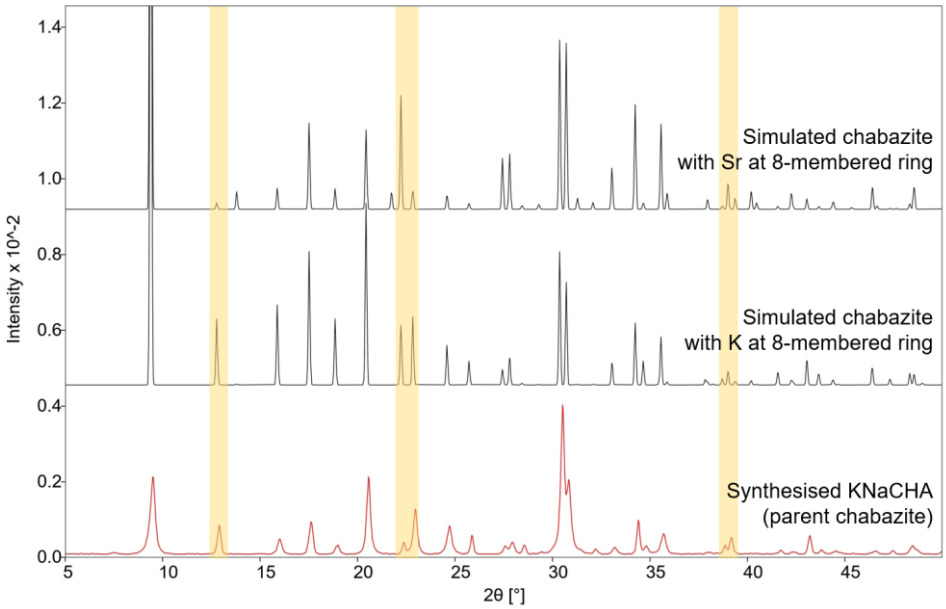

Figure S4. PXRD patterns of simulated K-CHA and simulated Sr-CHA (K and Sr positioned at the eight-membered ring) in comparison to PXRD pattern of synthesised KNa-CHA.

2.4. Solid-state magic-angle spinning nuclear magnetic resonance

^{29}Si NMR:

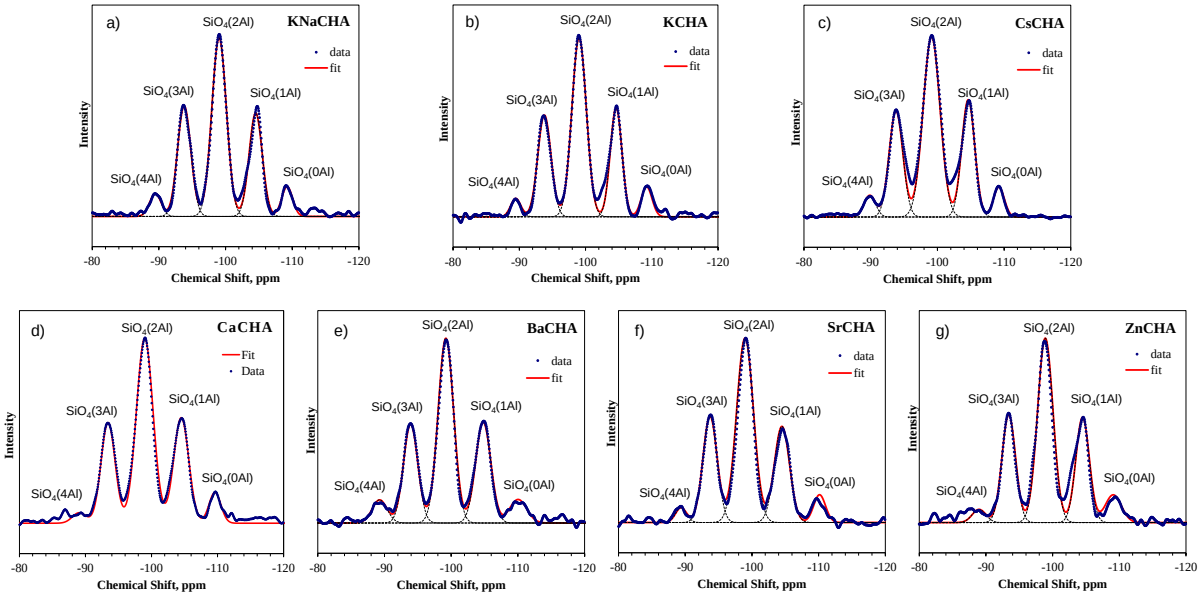

Figure S5. ^{29}Si NMR results of all chabazite zeolites

KNa-CHA: ^{29}Si NMR (79 MHz, none) δ ppm -108.85 (br. s., 2 Si) -104.63 (br. s., 10 Si) -98.93 (br. s., 19 Si) -93.48 (br. s., 11 Si) -89.26 (br. s., 2 Si). K-CHA: ^{29}Si NMR (79 MHz, none) δ ppm -109.10 (br. s., 3 Si) -104.63 (br. s., 23 Si) -98.68 (br. s., 47 Si) -93.48 (br. s., 25 Si) -89.51 (br. s., 4 Si). Cs-CHA: ^{29}Si NMR (79 MHz, none) δ ppm -108.85 (br. s., 7 Si) -104.39 (br. s., 28 Si) -98.68 (br. s., 42 Si) -93.48 (br. s., 18 Si) -89.26 (br. s., 3 Si). Ca-CHA: ^{29}Si NMR (79 MHz, none) δ ppm -109.59 (br. s., 2 Si) -104.39 (br. s., 22 Si) -98.68 (br. s., 49 Si) -93.23 (br. s., 26 Si) -89.26 (br. s., 3 Si). Ba-CHA: ^{29}Si NMR (79 MHz, none) δ ppm -109.59 (br. s., 3 Si) -104.63 (br. s., 24 Si) -99.18 (br. s., 46 Si) -93.72 (br. s., 27 Si) -88.52 (br. s., 2 Si). Sr-CHA: ^{29}Si NMR (79 MHz, none) δ ppm -109.59 (br. s., 2 Si) -104.39 (br. s., 21 Si) -98.93 (br. s., 47 Si) -93.48 (br. s., 28 Si) -89.01 (br. s., 3 Si). Zn-CHA: ^{29}Si NMR (79 MHz, none) δ ppm -109.35 (br. s., 4 Si) -104.39 (br. s., 25 Si) -98.68 (br. s., 46 Si) -93.23 (br. s., 25 Si) -89.73 - -85.33 (m, 2 Si).

Table S4. The chemical shifts from ^{29}Si and calculated Si/Al ratios of chabazite zeolites

Samples	SiO_4(0Al)	SiO_4(1Al)	SiO_4(2Al)	SiO_4(3Al)	SiO_4(4Al)	Si/Al
KNa-CHA	-109.2	-104.5	-99.0	-93.8	-89.5	2.00
K-CHA	-109.4	-104.5	-99.0	-93.8	-89.5	2.00
Cs-CHA	-109.2	-104.6	-99.2	-94.0	-89.8	2.04
Ca-CHA	-109.7	-104.4	-98.9	-93.5	-87.9	2.10
Ba-CHA	-110.1	-104.8	-99.2	-93.9	-89.3	2.06
Sr-CHA	-109.8	-104.6	-99.0	-93.8	-89.2	2.04
Zn-CHA	-109.4	-104.2	-98.8	-93.4	-87.9	2.08

^{27}Al NMR:

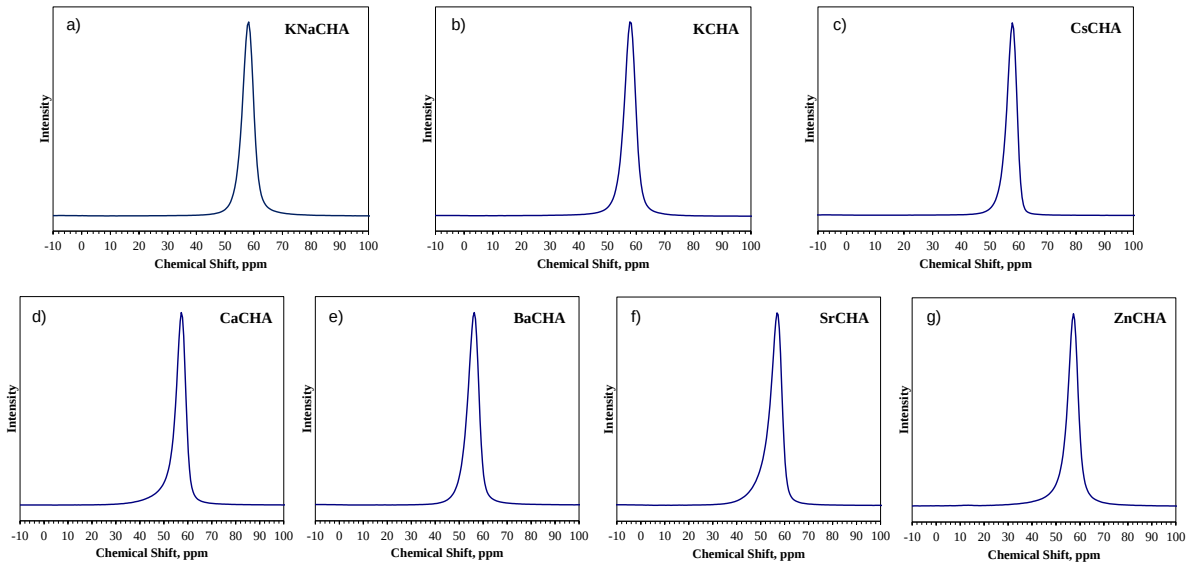

Figure S6. ^{27}Al NMR results of all chabazite zeolites

KNA-CHA: ^{27}Al NMR (104 MHz, none) δ ppm 58.29 (br. s., 160 Al). K-CHA: ^{27}Al NMR (104 MHz, none) δ ppm 57.80 (br. s., 69 Al). Cs-CHA: ^{27}Al NMR (104 MHz, none) δ ppm 57.80 (br. s., 98 Al). Ca-CHA: ^{27}Al NMR (104 MHz, none) δ ppm 57.31 (br. s., 97 Al). Ba-CHA: ^{27}Al NMR (104 MHz, none) δ ppm 56.33 (br. s., 98 Al). Sr-CHA: ^{27}Al NMR (104 MHz, none) δ ppm 56.82 (br. s., 98 Al). Zn-CHA: ^{27}Al NMR (104 MHz, none) δ ppm 57.31 (br. s., 100 Al).

Table S5. Chemical shifts from ^{27}Al of chabazite zeolites

Samples	KNa-CHA	K-CHA	Cs-CHA	Ca-CHA	Ba-CHA	Sr-CHA	Zn-CHA
Chemical shifts, ppm	58.26	58.26	57.77	57.28	56.30	56.79	57.28

2.5. Gas sorption

Table S6. Nitrogen sorption data of all chabazite zeolites

Samples	BET surface area (m^2 g^{-1})	Langmuir surface area (m^2 g^{-1})	t-plot micropore area (m^2 g^{-1})	BJH desorption pore volume (cm^3 g^{-1})
KNa-CHA	7.6	13.9	13.7	0.024
Cs-CHA	17.4	58.3	4.6	0.044
Ca-CHA	529.5	780.0	494.3	0.067
Ba-CHA	376.0	574.3	345.0	0.061
Sr-CHA	471.4	698.7	441.3	0.054
Zn-CHA	337.1	535.1	305.0	0.087

2.6. Powder X-ray diffraction of exchanged chabazite zeolites after gas sorption

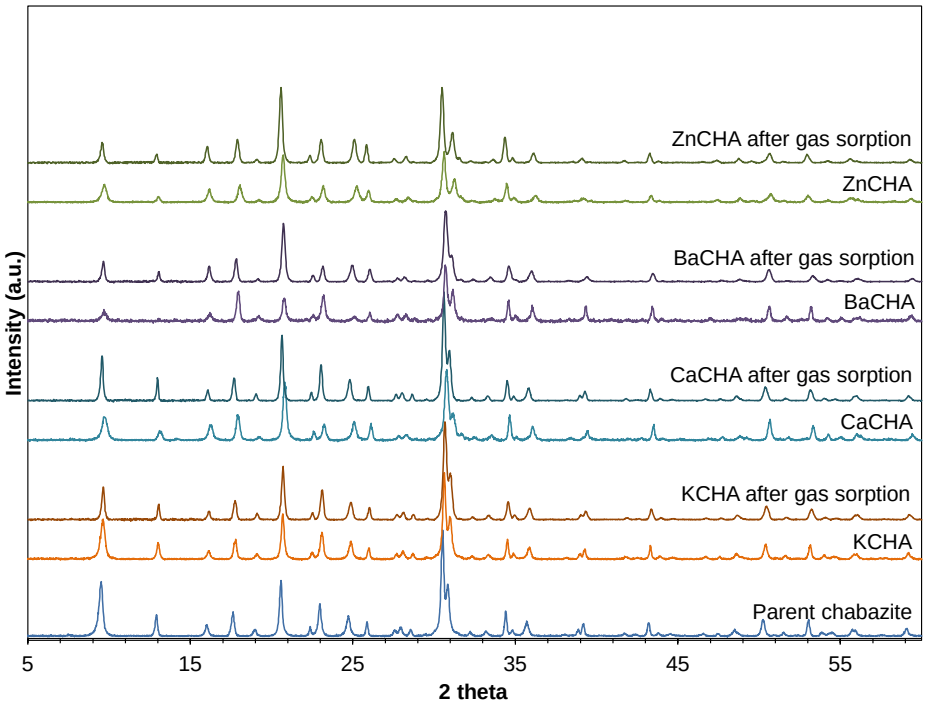

Figure S7. PXRD results of exchanged chabazite zeolites after gas sorption

References

1 M. Calligaris, G. Nardin and L. Randaccio, *Zeolites*, 1983, **3**, 205–208.

2 L. Lutterotti, M. Bortolotti, G. Ischia, I. Lonardelli and H.-R. Wenk, in *Tenth European Powder Diffraction Conference*, OLDENBOURG WISSENSCHAFTSVERLAG, 2015.